Temple University

Annual Progress Report: 2012 Formula Grant

Reporting Period

July 1, 2013 – June 30, 2014

Formula Grant Overview

Temple University received $2,220,937 in formula funds for the grant award period January 1, 2013 through December 31, 2016. Accomplishments for the reporting period are described below.

Research Project 1: Project Title and Purpose

Grand-Aides in Reducing Re-admission of Heart Failure Patients – Nationally, patients admitted to the hospital for exacerbation of heart failure symptoms have a 38% chance of readmission to the hospital within 60 days of discharge. At Temple, the rate of readmission for heart failure is as high as 34.7% within 30 days of discharge. Grand-Aides program combines trained community-based workforce and iPAD technology to provide improved access to care, optimal follow-up, and at a lower cost. We propose a randomized controlled trial to compare 30-day hospital readmission rates of heart failure patients assigned to conventional discharge care and follow-up, with those assigned to the Grand-Aides program. Our hypothesis is that 30-day readmission rates will be lowered by 30% with Grand-Aides.

Anticipated Duration of Project

1/1/2013 – 12/31/2016

Project Overview

Access to appropriate health care is inadequate and getting worse. In the United States shortages of 100,000 physicians and up to 1 million nurses are projected in the next 10 years; professional schools will only produce a fraction of these numbers. Transition of care from inpatient to outpatient care is of particular concern when talking about improving the efficiency and financial stability of the health care enterprise. Approximately 20% of Medicare beneficiaries who are discharged from the hospital are readmitted within 30 days, and over 30% are re-hospitalized within 90 days. The majority of these readmissions are unplanned, and many are likely preventable. The cost of these unplanned hospitalizations exceeds $17 billion annually.

Nationally, the 60-day readmission rate for heart failure patients is ~38% (New Eng J Med 367:2296-2305, 2012). At Temple serving a large cadre of underserved minorities, the 30-day readmission rate for heart failure patients is much higher at 34.7%. We propose to reduce the 30-day readmission rate by 30%, using Grand Aides, who are minimally trained community

health care workers with specific training in heart failure (Health Affairs 31:1016-1021, 2012). We will perform a controlled trial enrolling 884 heart failure patients discharged from Temple, and randomized to either receiving conventional discharge and follow-up care or visits and care by Grand Aides.

There are 2 Specific Aims:

Specific Aim 1**:** To randomize 884 patients with a discharge diagnosis of congestive heart failure into either conventional discharge and follow-up care or to Grand-Aides Program; and to analyze the results on 30 day re-admission rate. The primary end-point is reduction in 30-day re-admission rate.

Specific Aim 2: To perform subgroup analyses to evaluate if Grand Aides Program benefits selected groups of heart failure patients (e.g., early stage heart failure, patients with diabetes mellitus or hypertension), but not others (e.g., late stage heart failure).

Principal Investigator

Arthur M. Feldman, MD, PhD
Executive Dean and Professor of Medicine
Temple University School of Medicine
3500 N. Broad Street, Rm. 1150
Philadelphia, PA 19140

Other Participating Researchers

Kathleen Reeves, MD – employed by Temple University School of Medicine

Expected Research Outcomes and Benefits

We will recruit 884 patients with discharge diagnosis of congestive heart failure over next three years, with 442 patients in each arm. We anticipate a significant increase in the number of patients from the North Philadelphia community will participate in this research project and a decrease in the time it takes for new technology and innovations (Grand-Aides) to transition from research trials to everyday use by community practitioners.

Benefits will include delivery of better and more cost-effective medical care to an underserved patient population, minimization of hospital re-admission rate, and significant cost savings (return on investment as high as $2.72 per $1 spent; savings of $2,498 per beneficiary per year).

Summary of Research Completed

Electronic Medical Record Implementation
The electronic medical record enhancements needed in Epic are completed and are all functioning well via IPAD communication. We are also functioning well regarding HIPAA appropriate documentation in RedCap from EPIC and IPAD obtained information to ensure appropriate data.

Institution and Payor Education

We have come to understand the importance of having the entire health system leadership as well as insurers invested in the project. With great dedication and effort we have held multiple education sessions with all stakeholders improving the buy in from the institution, the faculty and payors. We have shared information regarding the lack of access to clinic research for populations like North Philadelphia and how this is a true health disparity and can have a negative effect on the health of people who live in communities like North Philadelphia. We have also shared how programs such as this can be tailored to be most beneficial to communities like North Philadelphia when we are able to incorporate specific community strengths and challenges into the programs. Having people from this community participate in the project is the only way this can be achieved. Finally we have spent significant time working with care providers including not only specialists but generalists as a patient's caregiver is the most important person to help encourage a patient to take part in any clinical research opportunity. All of these efforts have recently led to a modest increase in enrollment with the probability for a more substantial increased recruitment.

Community Outreach and Education

We have been accessing our community advisors as well as other community leaders through our active community engagement process to be sure that the community is aware of and willing to take part in the program. This process involves a multipronged approach dedicated to specific geographic neighborhoods. We have engaged in an ongoing, sustained presence that includes a presence in their schools supporting youth and a coordinated effort to help decrease violence. Though not directly related to this program, these two areas of engagement are the two most often identified by North Philadelphians and most important to them. We are also working on health education, flu shot provision, insurance education and access to primary and specialty care for all residents.

Study Implementation

As of today, we have 50 enrolled. This study is one of the first of its kind implemented in North Philadelphia. Our slow, initial recruitment has led to our community and stakeholder engagement noted above. We are blinded to the results of the study to date to ensure scientific integrity so can only comment on the number enrolled. We have also started a specific program looking at who should be obtaining consent and how this should be done. To date we have about an overall 25% consent rate. The initial proposal, based on recommendations from researchers within the Heart Failure group at Temple, assumed an 85% consent rate. We have realized there are certain techniques and certain individuals who are more successful obtaining consent. Concentrating on these researchers and their techniques along with the community engagement plans will help us significantly increase the number of enrolled patients.

Additionally, substance abuse including alcohol use prevents patients from being included in the study. Initially it was thought that such substance misuse was seen in as many as 25% of the eligible patients. We are currently documenting a rate of >60% of eligible patients who are being excluded because of substance misuse. We are working with the IRB and cardiology team to change the inclusion criteria to include some of these patients with less severe substance misuse issues. This will also increase our enrollment.

We are tracking enrolled patients based on the New York Heart Failure classification as well as according to age, sex, self-designated ethnicity, literacy level, education level, economic well-being, quality of life, and social support structure. We are also following comorbid conditions including but not limited to diabetes, hypertension, renal disease, and obesity.

Research Project 2: Project Title and Purpose

Protein Kinase A Inhibition and Heart Failure – Heart failure (HF) is a lethal syndrome characterized with progressive cardiac function depression, reduced exercise capacity, decreased cardiac reserve and blunted adrenergic responsiveness. Myocardial infarction (MI) is a major cause of HF. The mechanisms responsible for the development of HF after MI are not entirely clear. The purpose of this project is to evaluate the roles of endogenous protein kinase A inhibitor peptide (PKI) in cardiac physiology and pathophysiology and the potential of using PKI as a novel way to prevent adverse cardiac remodeling after myocardial infarction (MI).

Duration of Project

1/1/2013 – 12/31/2013

Project Overview

The project evaluates the roles of endogenous protein kinase A inhibitor peptide (PKI) in cardiac physiology and pathophysiology and the potential of using PKI as a novel way to prevent adverse cardiac remodeling after myocardial infarction (MI). We hypothesize that PKI-mediated inhibition of excessive PKA activation in stressed hearts will reduce the potentially detrimental effects of PKA and CaMKII signaling and will preserve beneficial effects of SAS signaling through cAMP/EPAC and β2AR/Gi/Akt pathways. To test these ideas, we have established a PKIα knockout mouse line, and transgenic mouse lines overexpressing different levels of a PKI-GFP fusion gene. To explore the role of EPAC activation in the improvement in cardiac structure and function caused by PKA inhibition after MI we will use mice deficient in EPAC1 or EPAC2. Our tools will allow us to dissect PKA-dependent and independent mechanisms of SAS signaling in heart failure.

SPECIFIC AIMS:
1) To determine the role of endogenous PKA inhibition by PKI in HF development after MI. PKIα knockout and control mice will be stressed with MI. The changes in PKI isoform expression, distribution, association with other signaling molecules in the signaling complex will be determined. The expression of genes related to Ca2+ handling, apoptosis and hypertrophy will be measured. These studies will define the role of endogenous PKI in normal and post-MI hearts.
2) To determine if and how selective inhibition of PKA, with overexpression of a PKI minigene, can reduce MI-induced structural and functional changes that cause HF. We will compare the protective effects of PKA inhibition with PKI to those of β-blockers. Specific experiments will:

a. Determine the appropriate level of cardiac specific expression of PKI (in transgenic mice or alternatively with AAV-mediated gene delivery), to induce gene dosage dependent PKA inhibition that reduces structural and functional defects caused by MI
b. Determine how PKA inhibition with PKI improves cardiac function after MI. First we will

focus on cAMP-dependent EPAC/Rap1/Raf/ERK and β2AR/Gi/PI3K/Akt cardio-protective signaling and CREB regulated gene expression;
c. Determine if PKA inhibition by PKI exerts more benefit than β-blockers providing comparable PKA inhibition on post-MI adverse cardiac remodeling.

Principal Investigator

Xiongwen Chen, PhD
Assistant Professor of Physiology
Temple University School of Medicine
3500 N. Broad Street, MERB-10
Philadelphia, PA 19140

Other Participating Researchers

None

Expected Research Outcomes and Benefits

The expected outcome is that we will be able to delineate novel mechanisms of regulation of post-infarction modeling and improve cardiac performance post-injury. The benefits of the research project are to utilize the new information to translate the research findings to the bedside in order to improve care of heart failure patients.

Summary of Research Completed

With the support from Pennsylvania Department of Health CURE funding, we have performed studies according to our original proposal focusing on the two specific aims as described below.

Specific Aim 1: To determine the role of endogenous PKA inhibition by PKI in HF development after MI. PKIα knockout and control mice will be stressed with MI. The changes in PKI isoform expression, distribution, association with other signaling molecules in the signaling complex will be determined. The expression of genes related to Ca^{2+} handling, apoptosis and hypertrophy will be measured. These studies will define the role of endogenous PKI in normal and post-MI hearts.

Progress: We first determined the expression of PKI α, β, and γ isoforms in post-myocardial infarction (MI) mouse hearts and failing human hearts with both real-time polymerase chain reaction (PCR) and Western blot. We found that the expression of PKIα but not PKIβ, γ is reduced. It seems that MI hearts were trying to enhance protein kinase A activity by decreasing PKA inhibitor to enhance cardiac β-adrenergic response.

Then we studied PKI isoform distribution by immunostaining in isolated mouse ventricular myocytes and we found that PKIα is evenly distributed in the ventricular myocyte but PKIβ and PKIγ are mostly on the sarcolemmal membrane.

We used PKIα knockout mice to explore the role of PKIα in cardiac physiology and pathology.

First, we studied if the loss of PKIα causes compensatory changes the expression of components of β-adrenergic system (βAR/adenylyl cyclase/PKA) and PKI isoforms. The loss of PKIα did not cause the change of the expression of other isoforms (PKIβ and PKIγ), nor did it change the expression of PKI catalytic subunits, PKA regulatory subunit Iα and Iβ, PKA regulatory RIIα, β1AR and β2AR. We also evaluated cardiac function and morphology with echocardiography in PKIα knockout mice and did not find difference in basal cardiac function and morphology. We also studied basal cardiomyocyte function between PKIα KO and control myocytes. Again, the data did not show significant differences between these two groups of myocytes. At the molecular level, we used Western blotting to determine if the loss of PKIα impacts on the abundance and phosphorylation level of Ca^{2+} handling proteins. We found that PKIα knockout mouse hearts had the same protein abundance of Ca^{2+} handling proteins as in control mouse hearts. Although the PKA-dependent phosphorylation of Ca^{2+} handling proteins tended to be greater in the PKIα knockout hearts, only the Ser16 phosphorylation in phospholamban (PLB) was significantly increased.

Then we studied whether the loss of the PKA inhibitor peptide enhances cardiac β-adrenergic responses in vivo with intra-left ventricle (LV) hemodynamic recording and ex vivo Langendorff perfused heart preparation. For in vivo intra-LV hemodynamic recording, different doses of isoproterenol (ISO, a β-adrenergic agonist) were infused into the circulating blood stream through a cannula inserted into the jugular vein. After each injection, two-minutes of recording was done. The data showed that the enhancement of heart rate, maximum +dp/dt (an index of contractility), minimum –dp/dt (an index of relaxation capability), developed pressure, contractility index and the tau for pressure decay by ISO was about 10 times more sensitive in PKIα KO mice than in control WT mice. Since our knockout of PKIα is global, we further tested the increased sensitivity to ISO stimulation is an intrinsic property of the PKIα knockout hearts by determining the responses of Langendorff perfused hearts to ISO stimulation ex vivo. The loss of PKIα rendered the heart to be more sensitive to ISO stimulation. Similar to what was seen in Langendorff perfused hearts, isolated ventricular myocytes from PKIα KO were more sensitive to ISO stimulation. A dose of 10nM ISO caused maximum effect on myocyte contraction, calcium transient and SR Ca2+ content in PKIα KO myocytes but a dose of 100nM ISO was needed to get the maximum effect in control myocytes. At the molecular level, 10nM ISO induced more PKA-dependent phosphorylation of phospholamban (PLB) at the Ser16 site and subsequent CaMKII phosphorylation of PLB at the Thr17 site in PKIα KO myocytes than in control myocytes.

Finally, we determined whether the loss of PKIα affects cardiac morphological and functional remodeling after myocardial infarction (MI). Myocardial infarction was surgically introduced in PKIα KO and control mice by ligating the left anterior descending coronary artery. Eight weeks after MI surgery, cardiac function and morphology were analyzed with echocardiography with Vevo 770 ultrasound machine and intra-LV hemodynamic measurement. After these procedures, the animals were weighed for body weight (BW) and killed and the heart was excised. Heart weight (HW) for each animal was recorded. Infarction size of hearts was measured with triphenyl tetrazolium chloride (TTC) staining. PKIα KO hearts developed more severe cardiac hypertrophy as implied by a greater HW/BW in PKIα KO MI mice than in control MI mice. The lung weight to body weight ration (LungW/BW) was also greater in post-MI PKIα KO mice than in post-MI control hearts, suggesting worse pulmonary edema and heart failure in PKIα KO

mice. The infarction size was nonsignificantly greater in post-MI PKIα KO hearts. Fractional shortening and ejection fraction were more reduced in post-MI PKIα KO hearts. When post-MI LV function was assessed by intra-LV hemodynamic measurements and the heart rate was controlled within the range of 400-450 beats per minute (BPM), post-MI PKIα KO mice had significantly higher end diastolic pressure (EDP), lower developed pressure, longer systolic duration but shorter diastolic duration, smaller maximum +dp/dt and more depressed minimum –dp/dt and contractility index than post-MI control mice. All these results suggest that although the loss of PKIα could enhance cardiac b-adrenergic response, it makes the heart more susceptible for myocardial infarction induced adverse cardiac functional and morphological remodeling.

Specific Aim 2: To determine if and how selective inhibition of PKA, with overexpression of a PKI minigene, can reduce MI-induced structural and functional changes that cause HF. We will compare the protective effects of PKA inhibition with PKI to those of β-blockers.

2a. Determine the appropriate level of cardiac specific expression of PKI (in transgenic mice or alternatively with AAV-mediated gene delivery), to induce gene dosage dependent PKA inhibition that reduces structural and functional defects caused by MI

Progress: We performed myocardial infarction (MI) surgery in low expression line and high expression line to determine the appropriate expression level of PKI-GFP offering cardiac protection. Mouse survival was observed. To our surprise, the low expression PKI-GFP transgenic (TG) mice subjected to myocardial infarction had lower survival rate than control mice. The high expression PKI-GFP TG mice had the same survival rate as the control mice. In another study group with PKI-GFP high expression line, almost all mice could not survive the myocardial infarction surgery, probably because the mice need β-adrenergic response to survive the initial insult. Therefore, in our further study, we used PKI-GFP TG medium expression (ME) mice as our experimental group.

At 8 weeks after MI, PKA inhibition did not significantly improve animal survival, probably due to high survival rates of animals in both control and TG groups, thanks to the improved MI procedure by Dr. Erhe Gao (Gao E et al., Circulation Research, 2010; 107(12): 1445-53). However, PKA inhibition reduced myocardial infarction size and end diastolic pressure, and increased +dp/dt and –dp/dt and cardiac diastolic duration. These results indicate moderate PKA inhibition is protective.

2b. Determine how PKA inhibition with PKI improves cardiac function after MI. First we will focus on cAMP-dependent EPAC/Rap1/Raf/ERK and β2AR/Gi/PI3K/Akt cardio-protective signaling and CREB regulated gene expression;

Progress: We have published a paper in Circulation Research in 2013 with our PKI-GFP ME mouse line showing that when PKA is inhibited by PKI-GFP in the heart, β-adrenergic stimulation induced cAMP production and subsequent EPAC activation. EPAC then activated ERK1/2 to protect myocytes from death. Therefore, our focus of this subaim is to test whether β2AR signaling plays a role in post-MI PKI-GFP TG mice. Our logic is that the main mediator for the detrimental effects of chronic β-adrenergic activation is PKA and when PKA is inhibited,

β2AR activation may switch its signaling to the protective Gi/PI3K/Akt signaling. Therefore, blocking β2AR signaling in post-MI hearts may reduce the beneficial effect of PKI. As predicted, β2AR antagonist ICI 118 551 decreased animal survival rate in both control and PKI-GFP ME TG mice, indicative of a protection offered by β2AR signaling.

2c. Determine if PKA inhibition by PKI exerts more benefit than β-blockers providing comparable PKA inhibition on post-MI adverse cardiac remodeling.

Progress: We introduced myocardial infarction in PKI-GFP ME TG mice and littermate control mice. Soon after the surgery, animals were treated with vehicle, 30mg/kg/day, 100mg/kg/day and 250mg/kg/day (i.p.) metoprolol. Animal survival was monitored during the 8-week observation period. At 8 weeks after MI, intra-LV hemodynamic measurements were done to evaluate cardiac function. We found that mouse survival was slightly better in PKI-GFP medium expression mice than in control mice. Metoprolol did not improve animal survival, instead, high dose of metoprolol significantly increased animal death rate in both PKI-GFP ME TG and control mouse groups. In terms of cardiac function, PKI-GFP medium expression protected hearts from cardiac function deterioration. This protection was even better than a dose of metoprolol (30mg/kg/day) protecting post-MI control mice. However, higher doses of metoprolol decreased cardiac function in both groups of mice.

Research Project 3: Project Title and Purpose

Therapeutic Potential of Myocyte Caveolae NO-cGMP Signaling in Cardiac Diastolic Dysfunction and Diastolic Heart Failure – Diastolic dysfunction—abnormal left ventricular (LV) diastolic relaxation, filling, and/or distensibility—characterizes one of the great challenges in cardiovascular medicine, heart failure with preserved ejection fraction (HFpEF). HFpEF accounts for more than half of chronic heart failure cases, yet evidence-based therapy for HFpEF is lacking. Our primary objective is to study the changes in myocyte caveolae NO-cGMP signaling with diastolic dysfunction, focusing on regulatory mechanisms of sGC activity and the functional implications of caveolae-localized NO-cGMP signaling.

Anticipated Duration of Project

1/1/2013 – 12/31/2014

Project Overview

Central Hypothesis: Disruption of caveolae-localized myocyte NO-cGMP signaling diminishes NO-mediated cardioprotection and NO-modulated cardiac relaxation, thereby causing diastolic dysfunction.

Using age-matched Fisher 344/Brown Norway F1 (F344/BNF1) and spontaneously hypertensive (SHR) rats, we will test this central hypothesis by pursuing these specific aims:
AIM 1. Determine if disruption of caveolae-based NO-cGMP signaling is associated with diastolic dysfunction in age-related and pathologic cardiac remodeling.
AIM 2. Determine whether and how restoring caveolae-localized NO-cGMP signaling in aged or

hypertrophied hearts rescues diastolic function.

Principal Investigator

Emily Tsai, MD, PhD
Assistant Professor of Medicine
Temple University School of Medicine
3500 N. Broad Street, MERB-10
Philadelphia, PA 19140

Other Participating Researchers

None

Expected Research Outcomes and Benefits

The expected outcome is that we will be able to delineate novel mechanisms underlying diastolic dysfunction. The benefits of the research project are to utilize the new information to translate the research findings to the bedside in order to improve care of cardiac patients.

Summary of Research Completed

Comparison of young (age 8 months) versus old (age 30 months) rats failed to show any significant difference in the intramyocardial distribution of the signaling proteins involved in direct nitric oxide (NO) signaling ---- soluble guanylyl cyclase (sGC), cyclic guanosine monophosphate (cGMP)-dependent protein kinase (PKG), or phosphodiesterase 5 (PDE5) between old and young hearts, suggesting that age-associated diastolic dysfunction may be distinct from pathologic diastolic dysfunction. Given these unexpected findings and the potentially limiting expense of aged rats, we turned to the chronically volume-overloaded heart, in which myocardial stiffness increases and filling rates decrease, as an alternative model of diastolic dysfunction. In collaboration with Dr. Louis Dell'Italia (University of Alabama at Birmingham), we studied the canine model of chronic mitral regurgitation. Dr. Dell'Italia is generously providing us with abundant cardiac tissue from control and chronic mitral regurgitation dogs.

Volume-overload was established by chordal rupture-induced mitral regurgitation (MR) in 16 dogs, which were analyzed at 2 weeks (N=6), 4weeks (N=5), and 12months (N=5) post-chordal rupture. Since our 2013 progress report, we published our findings on differential dysregulation of myocardial sGC in 4wk MR (n=5) and 12mo MR (n=5) versus unoperated controls (n=5) in the *Journal of Molecular and Cellular Cardiology*. In brief, sGC α_1 and β_1 subunits were distributed within plasmalemmal caveolae membrane microdomains as well as heavy-density, non-lipid raft membrane fractions in the normal heart. However, sGC heterodimer subunits moved away from caveolae at different stages of volume-overload induced eccentric hypertrophy. At 4wkMR, when left ventricular systolic function was still preserved, sGC β_1 relocalized away from caveolae, while sGCα_1 remained within caveolae. By 12moMR, sGCα_1

also relocalized outside of caveolae. At both compensated (4wkMR) and decompensated (12moMR) stages of eccentric hypertrophy, sGC within the heavy-density, non-lipid raft membrane fractions was oxidized. Caveolae-localized sGC appeared protected against oxidation. At 12moMR, myocardial expression of both sGC subunits fell and NO-responsiveness of sGC was likewise depressed within NLR. The differential spatiotemporal regulation of myocardial sGC subunits in this canine model also afflicted with diastolic dysfunction suggests that dissociation of sGCβ_1 from caveolae may correspond with diastolic dysfunction.

Our most recent findings of the effect of chronic β_1-adrenergic blockade with metoprolol succinate therapy on myocardial sGC regulation and NO-cGMP signaling in the canine chronic MR model also supports the hypothesis that caveolae-localized sGCβ_1 may contribute to normal diastolic function. Dogs subjected to chordal-rupture induced mitral regurgitation and treated with twice daily metoprolol succinate had preserved caveolae-localization of sGCβ_1. Echocardiographic parameters of diastolic function remain to be fully analyzed in these animals.

As for studies relevant to Aim 2, we have been working on generating cardiotropic adeno-associated virus and adenovirus carrying a caveolae-targeted sGCβ_1 construct. These were intended for *in vivo* gene transfer in animal models of diastolic dysfunction as well as *in vitro* cell culture studies. We have been able to identify a specific clone with good expression of sGCβ_1 and are moving forward with the AAV production. We will likely also synthesize another construct whereby the caveolin binding domain is at the N-terminus, rather than the C-terminus.

Research Project 4: Project Title and Purpose

Vasopressin 1A Receptor and Heart Failure – The progression of heart failure (HF), a disease that affects over 5 million individuals in the U.S. alone, is mediated in part by the release of neurohormonal signals and subsequent activation of G protein-coupled receptors. Arginine vasopressin (AVP) is a neurohormone that modulates cardiovascular function through activation of AVP type 2 receptors in the kidney and AVP type 1A receptors (V1AR) in the heart and vasculature. AVP levels are elevated in patients with HF and increased AVP levels are associated with increased morbidity and mortality. Little is known about AVP signaling in the heart. Our studies will elucidate the role of V1AR in HF progression and form the foundation for novel and rational HF therapy targeted at biased V1AR signaling.

Anticipated Duration of Project

11/26/2013 – 6/30/2015

Project Overview

Recent findings in the clinical heart failure (HF) literature indicate: 1) Arginine vasopressin (AVP) levels are elevated in patients with HF; 2) increased AVP levels are associated with increased morbidity and mortality; 3) the use of FDA-approved vasopressin receptor type 2 (V2R)-selective antagonists increases blood levels of AVP; and 4) the use of a V2R antagonist in patients with acutely decompensated HF was associated with an increase in mortality. We have

recently demonstrated that vasopressin receptor type 1A [V1AR; a G-protein coupled receptor (GPCR)] levels are increased 2x in hearts from patients with end-stage HF. In addition, cardiac-specific overexpression of the V1AR produced profound hypertrophy, fibrosis and diminished left ventricular function, a process mediated through $G_{\alpha q}$ protein-dependent signaling. These results led us to hypothesize that AVP signaling plays an important role in the progression of HF and that the V1AR could serve as a significant target for therapeutic intervention. However, there is a paucity of information regarding V1AR signaling and therefore a platform for rational drug discovery does not exist. Recent efforts to better understand the capacity of GPCR signaling to preserve, rather than diminish, cardiac function during HF have focused on G protein-independent signaling via G protein receptor kinase (GRK)/β-arrestin (βarr)-dependent signaling. We hypothesize that while chronic V1AR activation promotes maladaptive remodeling through $G_{\alpha q}$ protein-dependent signaling, GRK/βarr-dependent V1AR signaling affords cardioprotection. Thus, our Specific Aim is: Determine the roles of specific GRK and β-arrestin isoforms in regulating V1AR signaling and the resulting impact of these events on cardiac function and survival normally and under conditions of stress. We will use neonatal and adult myocytes in culture and ex vivo Langendorff perfused hearts. There are 3 SubAims: 1.1) Determine the isoform-specific impact of GRKs and β-arrestins on acute V1AR-dependent signaling responses in cardiomyocytes; 1.2) Determine the impact of GRK/βarr-dependent V1AR signaling on cardiac injury ex vivo; and 1.3) Determine the impact of V1AR expression in the progression of HF in vivo.

Principal Investigator

Arthur M. Feldman, MD, PhD
Professor of Medicine
Temple University School of Medicine
3500 N. Broad Street, MERB-1150
Philadelphia, PA 19140

Other Participating Researchers

Weizhong Zhu, PhD; Valerie Myers, BS – employed by Temple University

Expected Research Outcomes and Benefits

The expected outcome is that we will be able to delineate novel pathways by which heart failure progression can be halted. The benefits of the research project are to utilize the new information to translate the research findings for targeted drug discovery to improve care of heart failure patients.

Summary of Research Completed

The V1AR-selective antagonist SR 49059 preserves cardiac contractile function and restores both V1AR and βAR expression levels during the development of pressure overload-induced hypertrophy in vivo

To determine whether changes in endogenous V1AR expression are associated with the

development of cardiomyopathy and βAR dysfunction, WT mice underwent trans-aortic constriction (TAC) in conjunction with osmotic minipump-mediated delivery of the V1AR-selective antagonist SR 49059. As expected, TAC decreased cardiac function as monitored by echocardiography, however co-administration of SR 49059 preserved both fractional shortening and ejection fraction. SR 49059 administration in sham-operated mice did not impact cardiac function. Cardiac V1AR and βAR expression were also assessed in each of the surgical and treatment groups via radioligand binding. Interestingly, TAC induced a significant 2-fold increase in V1AR expression, similar to that observed in human hearts, which was inhibited by SR 49059. Interestingly, concomitant treatment of TAC mice with SR 49059 completely restored cardiac βAR expression to normal levels. These results confirm the involvement of endogenous V1AR signaling in the progression of heart failure and indicates that a loss of βAR density in the presence of chronically enhanced V1AR expression may account for the diminished βAR responsiveness we previously observed in V1AR-TG mice.

AVP negatively regulates endogenous cardiac βAR activation

To begin to understand a possible influence of cardiac-expressed V1AR on βAR signaling more acutely, we began to study the molecular relationship between these receptors. Initially, we performed [^{125}I] cyanopindolol (^{125}I-CYP) competition binding analysis with increasing concentrations of isoproterenol (ISO) ± AVP in membrane preparations from the hearts of adult mice. Although AVP alone did not alter ^{125}I-CYP binding to βAR, the addition of AVP induced a significant rightward shift in the ability of ISO to displace ^{125}I-CYP from βAR (IC_{50} of ISO from 0.14μM to 1.4μM, $p<0.0001$ (2-tailed t-test), indicative of a loss in affinity of βAR for ISO. Since Gs protein-dependent Ca^{2+} mobilization is enhanced downstream of βAR in cardiomyocytes, we measured field stimulation-induced Ca^{2+} transient responses in Fura2-loaded adult mouse left ventricular myocytes in the presence or absence of AVP and ISO). AVP alone did not alter Ca^{2+} handling even at μmolar concentrations, while ISO alone induced a substantial increase in the magnitude of the Ca^{2+} transients. Although, AVP did not evoke a change in Ca^{2+} mobilization alone, ISO-induced Ca^{2+} transients were significantly reduced in the presence of AVP.

βAR-induced Ca^{2+} transients occur in response to Gs protein-dependent generation of cAMP, thus we tested whether AVP stimulation impacts ISO-mediated cAMP production in adult feline left ventricular myocytes (AFVM) infected with adenovirus encoding the fluorescent cAMP biosensor ICUE3. Stimulation of AFVM with ISO produced only a small increase in cAMP production. Since βAR-dependent cAMP signaling is tightly controlled by phosphodiesterase 4 (PDE4) variants, we pretreated AFVM with the PDE4-selective antagonist rolipram to unmask the signal. Indeed, pretreatment of the cells with rolipram greatly enhanced the ISO-induced cAMP generation detected. Treatment of AFVM with AVP 1 min prior to ISO addition blocked the cAMP response regardless of PDE4 inhibition, suggesting that V1AR stimulation impacts βAR signaling at least at the level of cAMP generation and not cAMP degradation. To test whether cAMP generation is altered by AVP, AFVM were stimulated with forskolin, a direct activator of adenylyl cyclase, in the absence or presence of AVP. Although AVP significantly reduced ISO-dependent cAMP generation, AVP did not alter the ability of AFVM to produce cAMP in response to direct activation of adenylyl cyclase, further suggesting that V1AR stimulation impacts βAR at the receptor-G protein level.

V1AR-mediated regulation of βAR signaling is Gq protein-independent

To assess the mechanism by which V1AR stimulation decreases βAR signaling, we used HEK 293 cells stably expressing β1AR and transiently expressing V1AR and either ICUE3 or the fluorescent DAG biosensor DAGR. In these cells, ISO stimulation rapidly enhanced cAMP production while AVP had no impact on cAMP production on its own. As observed in AFVM, AVP pretreatment greatly reduced the ISO-mediated cAMP production, and similar to the binding data above, AVP induced a competitive rightward shift in ISO-mediated cAMP generation, altering the EC_{50} of ISO-dependent cAMP generation from 43pM to 256pM. To confirm that AVP effects on βAR signaling occur through V1AR, cells were pretreated with the V1AR-selective antagonist SR 49059. SR 49059 completely blocked AVP-dependent DAG production and did not prevent ISO-mediated cAMP production in the absence of AVP. However, SR 49059 pretreatment was able to restore ISO-dependent cAMP production in the presence of AVP. We then investigated whether V1AR-Gq protein signaling accounted for the effects of AVP on βAR-mediated cAMP generation. Although AVP signaling through V1AR negatively regulates β1AR-dependent cAMP formation, it does so in a Gq protein-independent manner. Indeed, transfection of HEK 293 cells stably expressing β1AR with either the wild-type (WT) V1AR or GRK$^-$V1AR mutant resulted in similar levels of membrane expression and affinity for AVP, while stimulation of the WT V1AR and GRK$^-$V1AR with AVP each induced rapid DAG formation, the GRK-V1AR caused a significantly greater accumulation of DAG, consistent with prolonged Gq protein-dependent activity of the receptor in the absence of GRK phosphorylation. Interestingly, AVP stimulation of GRK$^-$V1AR did not decrease βAR-dependent cAMP production, rather GRK$^-$V1AR stimulation significantly enhanced the ISO-mediated cAMP formation response. This effect was blocked by UBO-QIC, suggesting that in the absence of GRK-dependent regulation of V1AR signaling, Gq protein-dependent V1AR signaling promotes βAR sensitivity to adrenergic stimulation. To assess the impact of V1AR signaling on βAR function in the whole heart, ex vivo Langendorff analysis was performed using WT versus V1AR-TG mouse hearts as well as WT hearts receiving only AVP. The results were consistent with the single cell studies that V1A mediates desensitization of βAR signaling via a novel Gq protein-independent, GRK-dependent mechanism. These findings have important implications for the treatment of patients with an acute exacerbation of heart failure.

Figures: (Note that Figures 2 and 5 are not included in this report.)

Figure 1

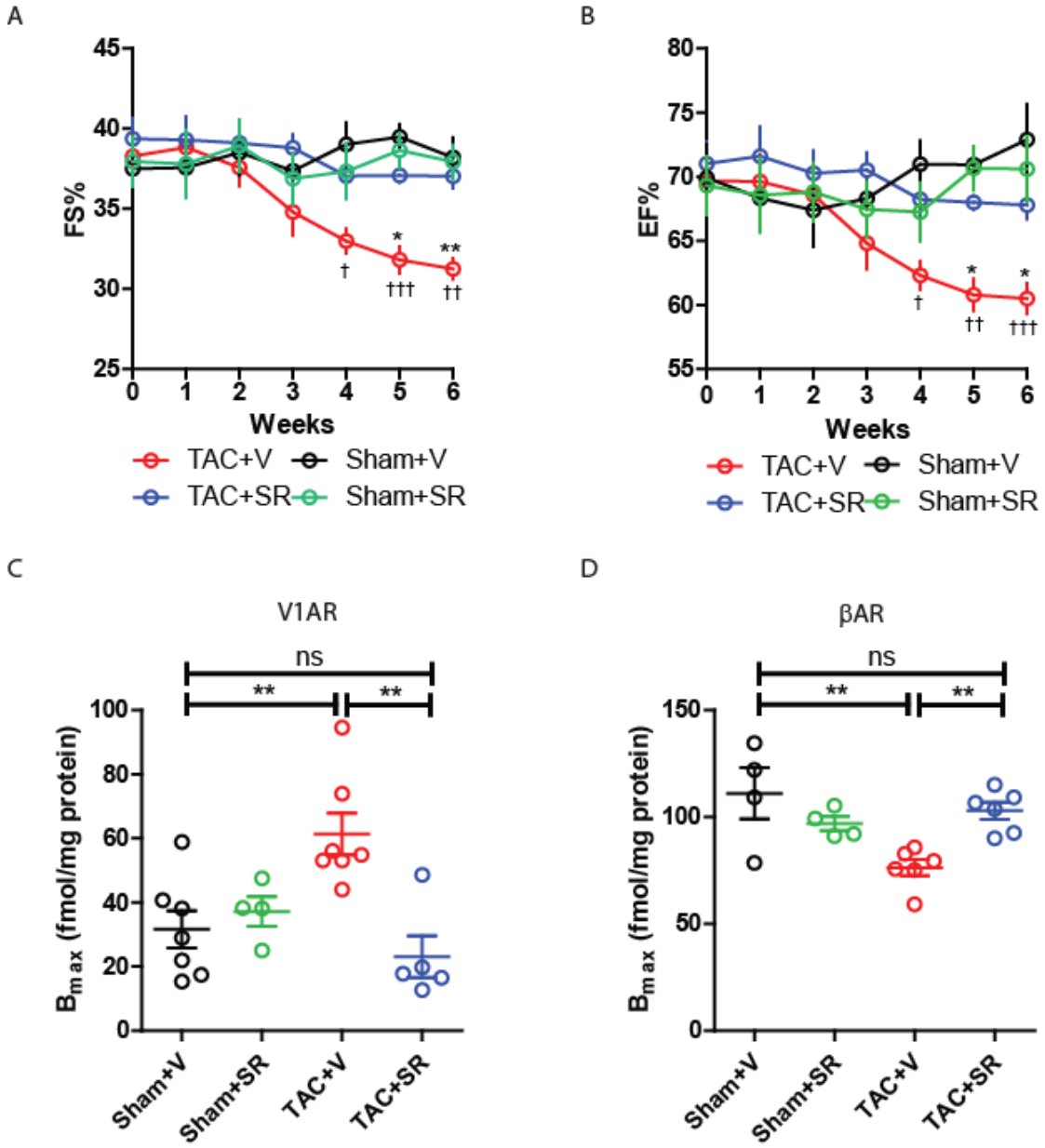

Figure 1. V1AR antagonist SR 49059 protects against TAC-induced cardiac dysfunction. In response to TAC, fractional shortening (A) and ejection fraction (B) were significantly decreased in vehicle-treated mice (TAC+V) compared to vehicle-treated sham surgery mice (Sham+V). Treatment of the TAC mice with SR 49059 (1mg/kg/day, starting 1 week post-TAC) prevented these changes. †p<0.05, ††p<0.01, †††p<0.001 versus Sham+V, *p<0.05, **p<0.01 versus TAC+SR at corresponding weeks, two-way ANOVA with Bonferonni multiple comparisons test. N = 9 (Sham+V), 8 (Sham+SR), 13 (TAC+V), 14 (TAC+SR). Radioligand binding analysis of left ventricular tissue of the Sham or TAC ± SR 49059 mice indicate that TAC increases V1AR membrane density (C, N = 7 (Sham+V), 4 (Sham+SR), 7 (TAC+V), 5 (TAC+SR)) and decreases βAR membrane density (D, N = 4 (Sham+V), 4 (Sham+SR), 6 (TAC+V), 6 (TAC+SR)), effects that are reversed by treatment with SR 49059. *p<0.05, **p<0.01, one-way ANOVA with Bonferonni multiple comparisons test.

Figure 3

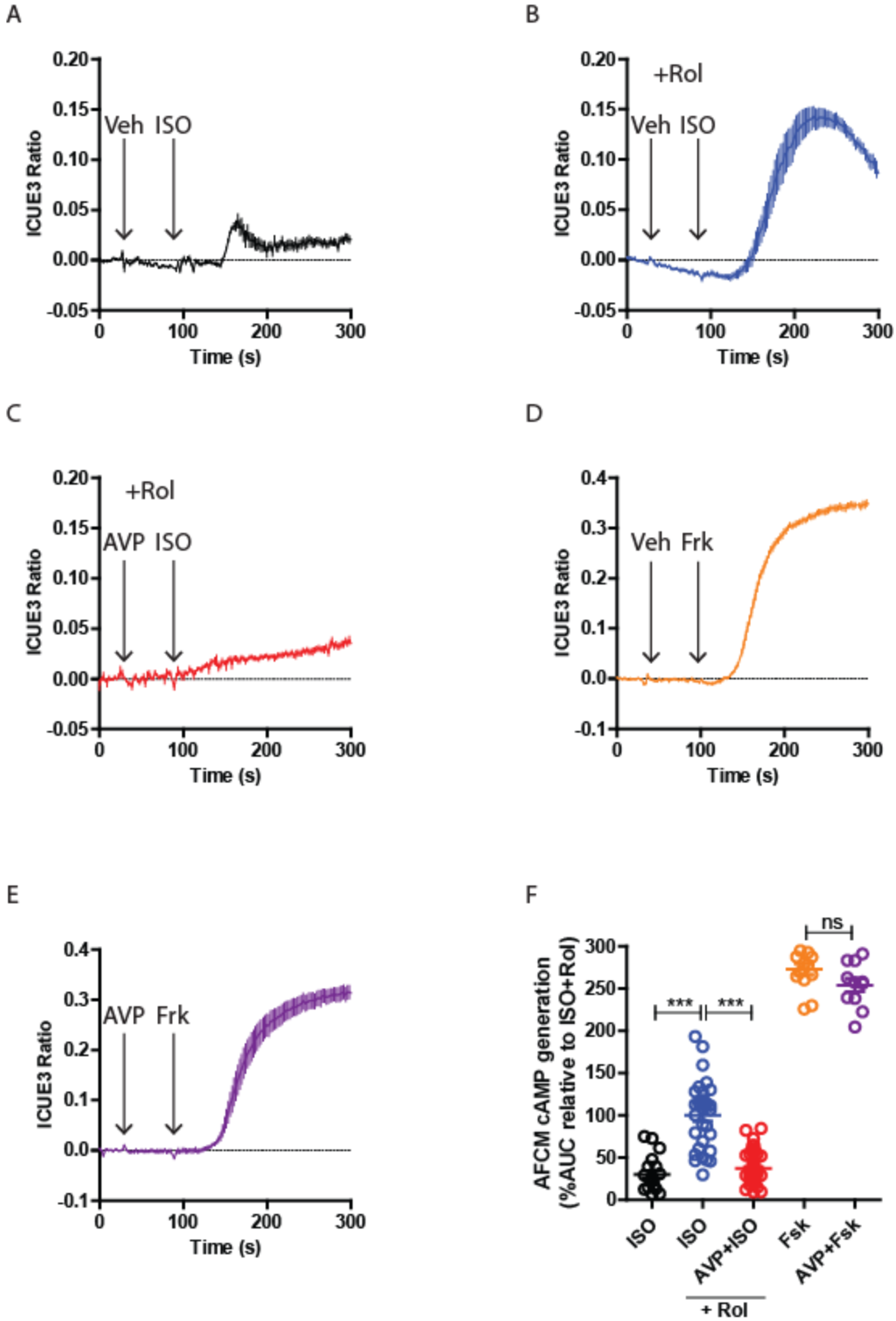
A
ICUE3 Ratio
Veh ISO
Time (s)
B
+Rol
Veh ISO
C
+Rol
AVP ISO
D
Veh Frk
E
AVP Frk
F
AFCM cAMP generation (%AUC relative to ISO+Rol)
ns
***
***
ISO
ISO
AVP+ISO
Fsk
AVP+Fsk
+ Rol

Figure 3. AVP reduces ISO-mediated cAMP generation in adult feline ventricular myocytes. cAMP generation responses were monitored in AFVM infected with the fluorescent biosensor ICUE3 in response to vehicle (Veh) + ISO (100 nM, A), rolipram (Rol, 1 µM) + Veh + ISO (B), Rol + AVP (1 µM) + ISO (C), Veh + forskolin (Frk 1 µM, D) or AVP + Frk (E). F) Summarized area under the curve (AUC) data relative to the Rol+ Veh+ ISO condition show that AVP pretreatment significantly reduces ISO-mediated cAMP generation, while not affecting Frk-mediated cAMP generation. ***$p<0.001$, one-way ANOVA with Bonferonni multiple comparisons test. N = 20 (ISO), 31 (Rol+ISO), 58 (Rol+AVP+ISO), 13 (Frk), 11 (AVP+Frk).

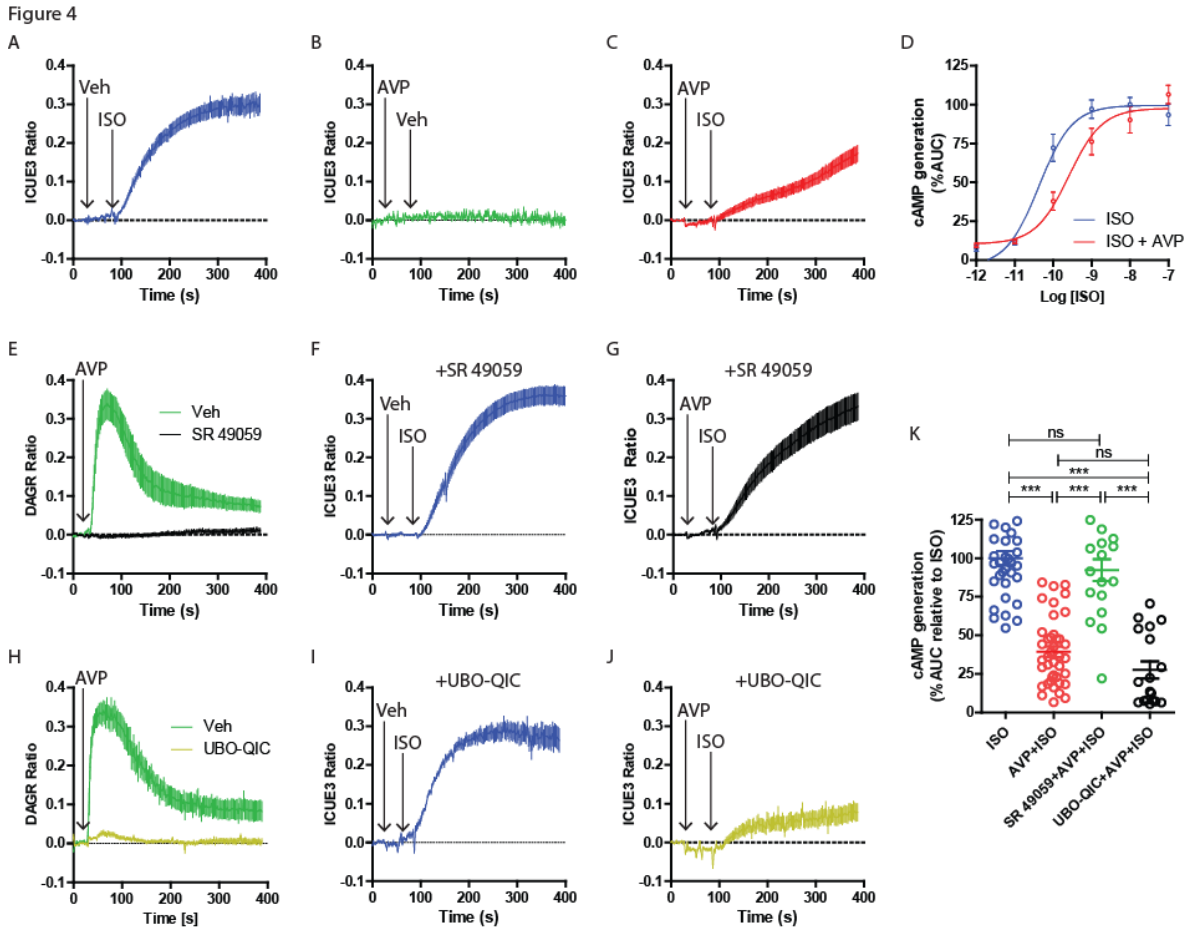

Figure 4. AVP effects on βAR-mediated cAMP generation are Gq protein-independent. cAMP and DAG generation responses were monitored in HEK 293 cells stably expressing β1AR and transiently transfected with V1AR and either ICUE3 or DAGR. Representative tracings show that ISO (100 pM, A) but not AVP (1 µM, B) increases cAMP generation. AVP pretreatment reduces ISO-mediated cAMP production (C) in a competitive manner (D). E) AVP (1 µM) induces a rapid DAG generation response that is blocked by SR 49059 (10 µM). Pretreatment of the cells with SR 49059 does not block ISO-induced cAMP generation (F) but does prevent the AVP-dependent reduction in the ISO response (G). H) The rapid DAG response to AVP stimulation is blocked by UBO-QIC (10 nM). Pretreatment of the cells with UBO-QIC neither blocks ISO-induced cAMP generation (I) nor the AVP-dependent reduction in the ISO response (J). K) Summarized area under the curve (AUC) results relative to ISO treatment alone, ***$p<0.001$, one-way ANOVA with Bonferonni multiple comparisons test. N = 34 (ISO), 40 (AVP+ISO), 18 (SR+AVP+ISO), 18 (QIC+AVP+ISO).

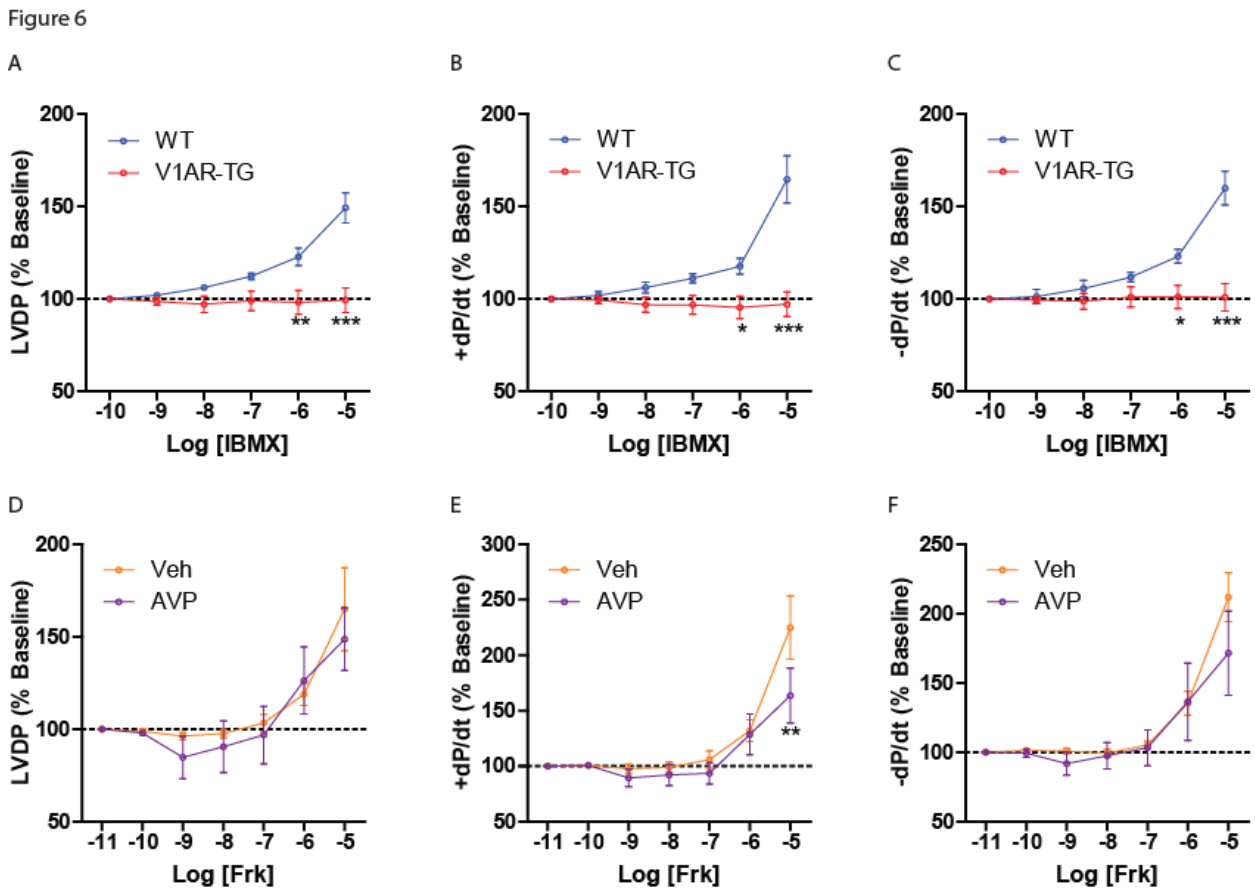

Figure 6. V1AR overexpression blocks basal cardiac contractility ex vivo, but V1AR activation does not impact adenylyl cyclase activity. Cardiac contractile parameters were measured in ex vivo Langendorff preparations from wild-type (WT) mice or mice with cardiac-restricted V1AR expression (V1AR-TG). Infusion of increasing concentrations of the non-selective phosphodiesterase inhibitor IBMX led to an increase in contractility in WT hearts as measured by LVDP (A), +dP/dt (B) and –dP/dt (C), expressed as % of baseline, effects that were absent in V1AR-TG hearts. *P<0.05, **P<0.01, ***p<0.001 versus WT hearts at corresponding concentration, two-way ANOVA with Bonferonni multiple comparisons test. N = 5 hearts each. WT hearts received increasing concentrations of the adenylyl cyclase activator forskolin (Frk), which enhanced LVDP (D), +dP/dt (E) and –dP/dt (F) in either the presence or absence of AVP (1 nM) pretreatment. **P<0.01 versus Veh-treated hearts at corresponding concentration, two-way ANOVA with Bonferonni multiple comparisons test. N = 5 hearts each.

Research Project 5: Project Title and Purpose

Transient Receptor Potential-Melastatin 2 (TRPM2) and Ischemic Heart Injury – TRPM2 channels are non-selective cation channels that are involved in cell proliferation and are emerging to be drug discovery targets for cancer therapy. In addition, TRPM2 channels are activated by ischemia. The physiological function of TRPM2 in the heart is unknown. We have generated a TRPM2-knock out mouse and observed that after ischemia-reperfusion injury or

doxorubicin (chemotherapeutic agent) treatment, cardiac function is significantly worse in TRPM2KO compared to wild-type hearts. The proposed studies are to elucidate cellular mechanisms by which TRPM2 channels protect hearts from ischemic and anthracycline injury. The results have significant impact on both ischemic heart disease and cancer chemotherapy.

Anticipated Duration of Project

11/26/2013 – 11/30/2014

Project Overview

TRPM2 is expressed in many tissues including heart, vasculature and hematopoietic cells, and has an essential role in susceptibility to oxidative stress and cell death. The function of TRPM2 in the heart is unknown. We are the first to demonstrate that TRPM2 is expressed in adult mouse LV myocytes, and that TRPM2 mediates $[Ca^{2+}]_i$ increase when myocytes are exposed to oxidative stress. After ischemia-reperfusion (I/R), TRPM2 knockout (KO) hearts had decreased function when compared to identically treated WT hearts. Our Overall Hypothesis is that TRPM2 channels protect hearts from oxidative damage. Understanding the function of TRPM2 in the heart therefore has high significance and clinical impact in that TRPM2 represents novel target to ameliorate ischemic heart injury. In addition, inhibiting TRPM2 is under development as an exciting new therapeutic approach for cancer. Combination chemotherapy in cancer frequently includes anthracyclines, and our preliminary observation that TRPM2KO mice treated with low dose doxorubicin exhibited additional myocardial dysfunction and markedly reduced survival compared to doxorubicin-treated WT mice, makes understanding of the functional roles of TRPM2 in the heart most timely and relevant.

Specific Aim 1: Is the protection afforded by TRPM2-mediated Ca^{2+} influx? We will express loss of function, increased Ca^{2+} selectivity, or inactivation TRPM2 mutants in KO myocytes to modulate TRPM2-mediated Ca^{2+} entry. Reactive oxygen species (ROS) generation by myocytes after hypoxia will be monitored as a surrogate for injury. Mutants will be expressed in KO hearts and the effects on in vivo ROS generation and cardiac function post-I/R evaluated.

Specific Aim 2: Is the protection due to better mitochondrial function and bioenergetics? Our proteonomics analysis strongly implicates mitochondrial dysfunction as a major contributing factor to worse cardiac function in KO mice post-I/R. We will determine the source of increased ROS: mitochondrial electron transport chain vs. NADPH oxidase (NOX). We will evaluate if eliminating ROS will be beneficial on mitochondrial function post-H/R. We will determine if enhanced ROS generation by TRPM2KO phagocytes contributes additional heart damage.

Principal Investigator

Joseph Y. Cheung, MD, PhD
Professor of Medicine
Temple University School of Medicine
3500 N. Broad Street, MERB-960
Philadelphia, PA 19140

Other Participating Researchers

JuFang Wang, MD; Xue-Qian Zhang, MD; Jianliang Song, MD, PhD – employed by Temple University

Expected Research Outcomes and Benefits

The expected outcome is that we will be able to delineate novel mechanisms by which TRPM2 channels protect the heart from ischemic injury and doxorubicin toxicity. The benefits of the research project are to utilize the new information to translate the research findings for targeted drug discovery to improve care of heart and cancer patients.

Summary of Research Completed

Methods

Generation of global (g) and cardiac-specific (c) TRPM2-KO mice. To generate cardiac-specific TRPM2 KO mice, exons 21 and 22 encoding TM domains 5 and 6 and the putative Ca^{2+} pore of TRPM2 gene were flanked by loxP recombination sites. $TRPM2^{fx/fx}$ mice (C57BL/6) were mated with αMHC-Cre (C57BL/6) mice to generate $TRPM2^{fx/+}Cre^{+/-}$ mice; which were mated with $TRPM2^{fx/fx}$ mice to generate the final desired progeny $TRPM2^{fx/fx}Cre^{+/-}$ and $TRPM2^{fx/fx}Cre^{-/-}$ mice served as WT. αMHC-Cre is expressed in the ventricle and atrium at around 1-2 days after birth. At 2 months of age, 64.0 ± 9.7% of floxed gene was deleted in hearts (5 cardiac-specific KO; 8 WT) as evaluated by qPCR. This likely represents the lower bound of TRPM2 deletion in cardiac myocytes since the whole heart contains fibroblasts, vascular endothelial cells and blood cells. In contrast, TRPM2 expression in cardiac-specific KO mice was not affected in bone marrow ($p<0.88$), brain ($p<0.94$) and liver when compared to WT.

Construction of TRPM2 and mutants. V5-tagged human TRPM2 in pAdTrack was used to generate the loss-of-function (E960D), inactivating (P1018L) and enhanced Ca^{2+} permeability (Q981E/P983Y) mutants using Altered Sites II in vitro mutagenesis system (Promega).

Isolation, adenoviral infection and culture of adult murine cardiac myocytes. Cardiac myocytes were isolated from the septum and LV free wall of WT and gKO mice (8-10 wks old), and plated on laminin-coated glass coverslips. Two hours after isolation, myocytes were infected with Adv-GFP (4.4×10^8 particles/ml), Adv-GFP-TRPM2 (1.6×10^8 particles/ml) or Adv-GFP-TRPM2 mutants (E960D 2.0×10^8; P1018L 4.5×10^8; Q981E/P983Y 3.75×10^8 particles/ml) in 5 ml of fetal bovine serum-free Eagle minimal essential medium (MEM) containing 0.2 % bovine serum albumin, creatine (5 mM), carnitine (2 mM), taurine (5 mM), $NaHCO_3$ (4.2 mM), penicillin (30 mg/L), gentamicin (4 mg/L), insulin-transferrin-selenium supplement and 2,3-butanedione monoxime (10 mM) for 3h. An additional 5 ml of MEM (with same supplements) was then added, and myocytes were cultured for 24h before measurements.

$[Na^+]_i$ measurements. Briefly, myocytes were exposed to 10 μM sodium-binding benzofuran isophthalate (SBFI) AM in the presence of Pluronic F127 (0.05% w/v) for 2h at 37ºC. Media was changed and myocytes were incubated for a further 30 min to allow de-esterification of the

AM ester. Measurements of $[Na^+]_i$ were performed in myocytes incubated in Tyrode's solution (37ºC) containing (in mM) 140 NaCl, 4 KCl, 1 $CaCl_2$, 10 glucose and 5 HEPES, pH 7.4. Dual excitation wavelengths (340 ± 15 and 380 ± 15 nm; alternating at 5 Hz) were directed to a single myocyte via a Nikon 40x/1.30 NA UV oil objective situated in a Nikon TE200U inverted microscope. Emission from a small area of the myocyte was recorded at 510 ± 40 nm.

Measurement of TRPM2 current in cultured myocytes. TRPM2 currents (I_{TRPM2}) were measured at 30°C in Adv-infected LV myocytes (cultured for 24h) with whole cell patch-clamp. Fire-polished pipettes (tip diameter 4-6 µm) were used. Pipette solution contained (in mM): CsCl 110, TEA.Cl 20, HEPES 10, EGTA 10, and MgATP 5, pH 7.2. To detect I_{TRPM2} inactivation (P1018L) and to estimate relative Ca^{2+} to Na^+ conductance (G_{Ca}/G_{Na})(Q981E/P983Y), cultured gKO myocytes expressing WT TRPM2 or its mutants were voltage-clamped at -80 mV. Extracellular solution contained (in mM): NaCl 140, HEPES 10 and glucose 15, pH 7.4. After break-in, inward Na^+ currents were obtained in gKO myocytes expressing WT TRPM2, P1018L or Q981E/P983Y mutant at -80, -90 and -100 mV. Extracellular solution was then changed to one containing (in mM): $CaCl_2$ 110, HEPES 10 and glucose 15, pH 7.4. Inward Ca^{2+} currents were obtained at -80, -90 and -100 mV from the same myocyte. G_{Ca}/G_{Na} is calculated from the ratio of the slopes of I-V plots with Ca^{2+} or Na^+ as the permeant ion.

Confocal mitochondrial superoxide (O_2-) measurement. Adult WT and gKO myocytes expressing GFP, TRPM2 or its mutants were loaded with the mitochondrial O_2- sensitive fluorophore MitoSOX Red (22 µM) in extracellular media (ECM) containing 2% BSA, 0.06% pluronic acid and 20 µM sulfinpyrazone at 37°C for 30 min. Cells were then washed, resuspended in ECM containing 0.25% BSA, and imaged using a Carl Zeiss Meta 510 confocal microscope with a 40x oil objective with 1.7x digital zoom at 561 nm for MitoSOX Red. In some experiments, gKO myocytes expressing GFP, TRPM2 or its mutants were subjected to 30 min of hypoxia (1% O_2-5% CO_2) followed by 30 min of reoxygenation (21% O_2-5%CO_2).

Ischemia-reperfusion (I/R) surgery in mice. Briefly, WT and cKO mice (8-10 weeks) were anesthetized with 2% isoflurane, and the heart was exposed through a left thoracotomy at the 5th intercostal space. The slipknot was tied around the left anterior descending coronary artery 2-3 mm from its origin, and the heart was immediately returned to the chest cavity followed by evacuation of pneumothorax and closure of muscle and skin layers. The slipknot was released after 30 min. of ischemia to allow reperfusion. Sham-operated animals were subjected to the same surgical procedure except that the slipknot was not tied. Animals recovered from anesthesia within 5 min. after the completion of surgery and received ibuprofen (10 mg/50 ml drinking water) for 48 h as post-surgery analgesia. Studies were performed on Day 3 post-surgery.

Statistics. All results are expressed as means ± SE. For analysis of +dP/dt as a function of group and isoproterenol, two-way ANOVA was used. For analysis of $[Na^+]_i$, ROS levels, and O_2 consumption, one-way ANOVA was used. A commercially available software package (JMP 7) was used. In all analyses, $p<0.05$ was taken to be statistically significant.

Results

Specific Aim 1

1. *H_2O_2 did not increase $[Na^+]_i$ in adult cardiac myocytes.* TRPM2 channels are permeable to both Ca^{2+} and Na^+. H_2O_2-induced $[Ca^{2+}]_i$ increase in WT myocytes could either be from direct Ca^{2+} entry, or secondarily from reverse Na^+/Ca^{2+} exchange (3 Na^+ out: 1 Ca^{2+} in) due to elevated $[Na^+]_i$. Treatment of WT and gKO myocytes with H_2O_2 did not change the F_{340}/F_{380} signal of the ratiometric dye SBFI (Fig. 1), indicating no detectable changes in $[Na^+]_i$ with H_2O_2. Therefore H_2O_2-induced increase in $[Ca^{2+}]_i$ was due to direct Ca^{2+} influx via activated TRPM2 channels.

2. *Electrophysiological phenotype of TRPM2 and its mutants.* We measured I_{TRPM2} in gKO myocytes expressing WT TRPM2, P1018L, E960D or Q981E/P983Y mutant by adenovirus-mediated gene transfer. I_{TRPM2} due to WT TRPM2 did not inactivate with time (Fig. 2). By contrast, P1018L mutant inactivated with time whereas E960D displayed no appreciable current elicited by intracellular ADPR (Fig. 2). G_{Ca}/G_{Na} in gKO myocytes expressing WT TRPM2 was 0.56 ± 0.02 (n=4; Fig. 2) and 1.06 ± 0.03 (n=3)($p<0.001$) in myocytes expressing Q981E/P983Y.

3. *TRPM2 but not E960D reduced elevated mitochondrial O_2- in gKO myocytes.* To evaluate whether lack of Ca^{2+} influx was the culprit in mitochondrial dysfunction in KO myocytes, we expressed WT TRPM2, loss-of-function E960D or inactivating P1018L mutants in gKO myocytes by adenovirus-mediated gene transfer. Compared to WT-GFP myocytes (Fig. 3A), gKO-GFP myocytes had ~5x mitochondrial O_2- levels (3B). Elevated mitochondrial O_2- in gKO-GFP myocytes were substantially reduced by expression of WT TRPM2 (3E) but not by the loss-of-function E960D mutant (3C). Overexpression of WT TRPM2 in WT myocytes had no effects on mitochondrial O_2- (3E). Interestingly, the inactivating P1018L mutant partially reduced mitochondrial O_2- (3D). These data suggest that Ca^{2+} entry via TRPM2 channels was necessary to rescue mitochondrial dysfunction in gKO myocytes under basal conditions.

4. *TRPM2 but not E960D reduced cardiac ROS and enhanced OCR in gKO hearts in vivo.* To evaluate if the beneficial effects of TRPM2 on cultured gKO myocytes could be translated in vivo, we expressed TRPM2 or E960D mutant in intact WT or gKO hearts by adenovirus-mediated gene transfer. Five days after Adv injection, significant portions of the LV exhibited GFP fluorescence, indicating successful transfer and expression of the exogenous gene. Heart slices that fluoresced green (Fig. 4A) were generated and in situ ROS and OCR were measured. gKO-GFP had much higher ROS levels (4B) and reduced OCR (4C) than WT-GFP heart slices. TRPM2 but not the loss-of-function E960D mutant rescued mitochondrial dysfunction in gKO hearts, as evidenced by reduced ROS (4B) and increased OCR (4C) back to WT levels.

Specific Aim 2

1. *Effects of I/R on cardiac performance in WT and cardiac-specific TRPM2 KO mice.* We have previously demonstrated that gKO mice have significant lower +dP/dt 3 days post-I/R when compared to WT mice. To ascertain whether the deleterious effects observed are due to absence of TRPM2 in the cardiac myocyte or other tissues such as phagocytes, we generated a cardiac-specific TRPM2 KO mouse. At 2 months of age, 64.0 ± 9.7% of floxed gene was deleted in hearts (5 cKO; 8 WT) as evaluated by qPCR. After I/R, cKO-I/R had significantly lower +dP/dt

when compared to WT-I/R hearts (Fig. 5). This strongly suggests that protective effects of TRPM2 are direct on cardiac myocytes rather than indirect through less inflammation.

2. *Ca^{2+} influx via TRPM2 was required for reduction of mitochondrial O_2- levels post-H/R.* To establish whether Ca^{2+} influx through TRPM2 was required for its protection against I/R injury, and as an independent approach to confirm the beneficial effects of cardiac TRPM2 on myocardial function post-I/R, we expressed GFP, TRPM2, E960D, P1018L or Q981E/P983Y mutant in gKO myocytes followed by H/R. Mitochondrial O_2- levels were used as a marker for mitochondrial dysfunction and by inference, cell injury. After 30 min of hypoxia followed by 30 min of reoxygenation, gKO-GFP myocytes exhibited high mitochondrial O_2- levels. TRPM2 or Q981E/P983Y but not E960D or P1018L mutant significantly lowered mitochondrial O_2- levels in gKO mycoytes post-H/R, indicating sustained Ca^{2+} influx through non-inactivating TRPM2 channels was required for protection against H/R injury. As an independent approach to evaluate the absolute requirement for Ca^{2+} entry, we conducted the H/R experiments in the absence of extracellular Ca^{2+} (no added Ca^{2+} + 4 mM EGTA). Absence of extracellular Ca^{2+} abolished the beneficial effects of WT TRPM2 on myocyte H/R injury.

Figures

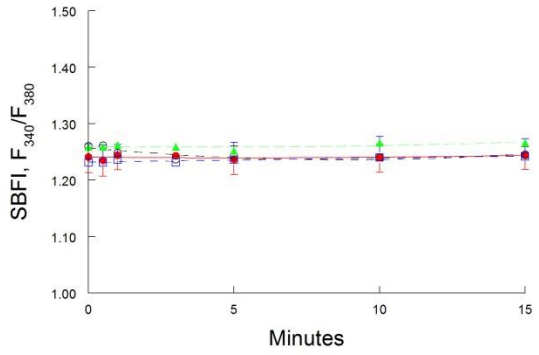

Figure 1. Activated TRPM2 channels do not increase intracellular Na^+ concentration $[Na^+]_i$ in adult mouse cardiac myocytes. SBFI-loaded myocytes were exposed to either H_2O_2 (200 µM) or control Tyrode's solution and $[Na^+]_i$ was measured at times indicated (Methods). There are 4 WT (open circles) and 4 KO (filled circles) myocytes exposed to H_2O_2 and 3 WT (open squares) and 2 KO (filled trianges) myocytes exposed to Tyrode's solution.

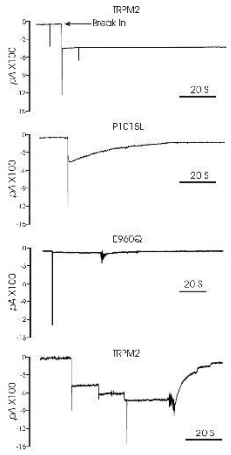

Figure 2. Cationic currents activated by ADPR in myocytes expressing WT TRPM2 or its mutants. TRPM2 knockout (gKO) myocytes expressing either TRPM2, P1018L, or E960D mutant by adenovirus-mediated gene transfer were held at -80 mV in 140 mM $[Na^+]_o$. ADPR (300 µM) was included in the pipette solution to activate TRPM2 channels after break-in (arrow). Representative TRPM2 current tracings for WT TRPM2, P1018L, and E960D are shown. In another gKO myocyte expressing WT TRPM2 bathed in 140 mM $[Na^+]_o$, after break-in, a large inward current that showed a linear increase with increasing hyperpolarization was observed. After medium change to one containing 110 mM $[Ca^{2+}]_o$, current became smaller and demonstrated a linear decrease with depolarization from -100 to -80 mV. G_{Ca} and G_{Na} were estimated from the slope of I-V relationship.

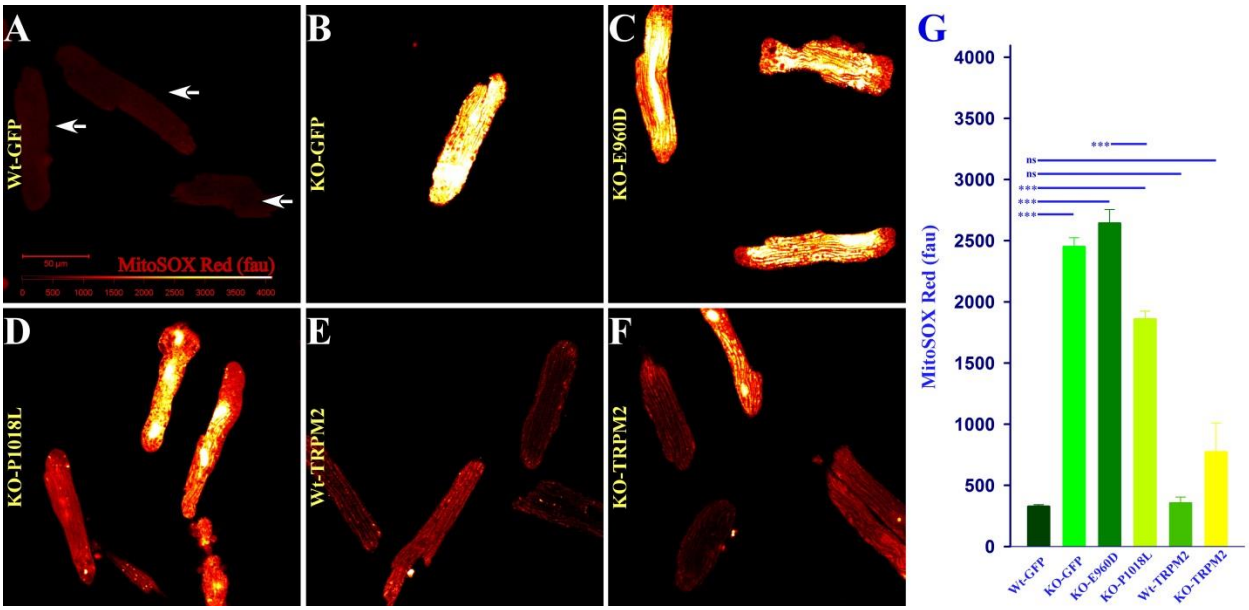

Figure 3. Elevated mitochondrial ROS levels in gKO myocytes are lowered by functional TRPM2 channels. MitoSox signals from WT or gKO myocytes expressing either GFP, TRPM2, E960D, or P1018L mutant are shown. Quantitation of MitoSOX Red signal intensities in fluorescence arbitrary units (fau). For each group, data are obtained from 10 random images totaling 20 to 30 cells. ***p<0.001.

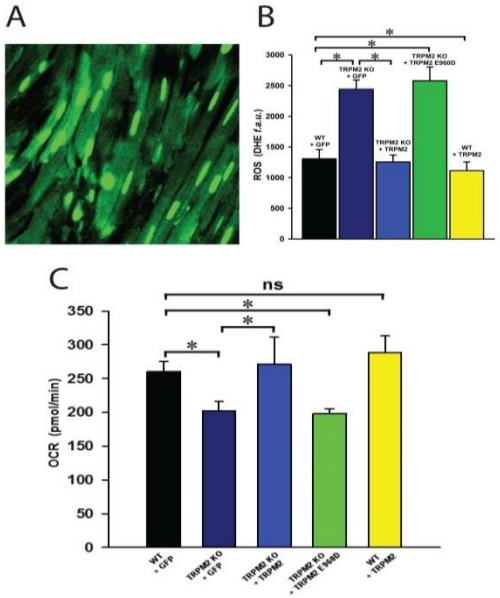

Figure 4. WT TRPM2 but not E960D reduces cardiac ROS and improves oxygen consumption rate (OCR) in heart slices in situ. (A). 5 days after injection of Adv-GFP, Adv-TRPM2, or Adv-E960D into hearts of WT or gKO mice, heart slices were generated from areas of LV exhibiting GFP fluorescence. (B). Multi-photon confocal images of dihydroethidium (DHE)-stained LV slices exhibiting GFP fluorescence were obtained, and DHE fluorescence in fau were quantitated. There are 8 slices from at least 2 hearts from WT-GFP, gKO-GFP, gKO-TRPM2, gKO-E960D and WT-TRPM2 animals. (C) LV heart slices generated as in (B) were subjected to OCR measurement. *p<0.05.

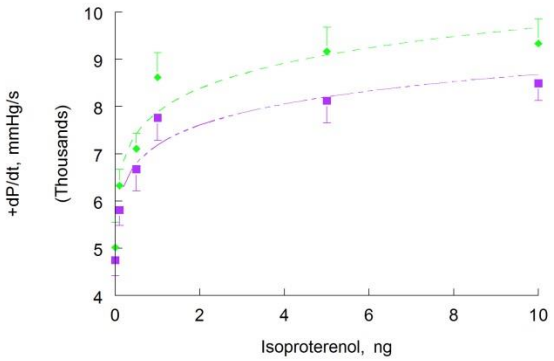

Figure 5. Cardiac performance after ischemia-reperfusion (I/R) is worse in cardiac-specific TRPM2 KO compared with WT hearts. Hearts were subjected to 30 min of ischemia followed by 3 days of reperfusion. In vivo catheterization was performed in anesthetized mice. +dP/dt was continuously measured, both at baseline and at increasing doses of isoproterenol. There were 8 WT-I/R (solid circles) and 12 cKO-I/R (filled rectangles) mice. Two-way ANOVA indicated p<0.005 for WT-I/R vs. cKO-I/R.

Research Project 6: Project Title and Purpose

Polydrug Use: Interactions between Cannabinoids, Opioids, and Nicotine – The purpose of this project is to study drug interactions among the systems that mediate addiction to nicotine, opioids and cannabinoids. All three classes of drugs are of major public heath interest because their use can lead to abuse and dependence. Substance abuse is a major public health problem in Pennsylvania and worldwide. Most people use more than one drug. This project will investigate polydrug interactions in preclinical rodent models to determine the effect of nicotine or cannabinoid exposure on cognitive parameters and pain responses to opioids. In addition, the role of the two major cannabinoid receptors, CB1 and CB2, will be evaluated to determine how each affects the polydrug interactions.

Anticipated Duration of Project

11/26/2013 - 6/30/2016

Project Overview

Most individuals who engage in substance abuse do not use only a single drug. Most smoke nicotine cigarettes in addition to using illegal substances. Adolescence is a period of particular vulnerability for drug use. This project will study how the various systems of the body that mediate the effects of nicotine, cannabinoids and opioids interact in adolescent animals. The role of the two cannabinoid receptors, CB1 and CB2, will be dissected in regard to their relative contributions to these interactive effects. Recently published studies provide evidence that the CB2 receptor can block rewarding effects of cocaine. New studies, including ones from our laboratory, show that the CB2 receptor mediates immunosuppression through its action on immune cells and microglia.

Specific Aims:
Aim 1: To determine the interactions of cannabinoids and opioids in terms of analgesia in two different pain models in rodents in the presence of inflammatory molecules produced by the immune system, called chemokines.
Aim 2: To identify the long-term effects of nicotine and cannabinoid (Δ^9-THC) exposure during adolescence as compared with adulthood, on cognition, anxiety, depression and sensitivity to the effects of opioids using a pre-clinical mouse model.

Aim 1 will investigate interactions between cannabinoids and opioids in two models of inflammatory pain in rodents. During pain with a high degree of inflammation, opioids have relatively poor efficacy, leading in some cases to use of higher doses of the drug that can result in addiction. Cannabinoids have been shown to reduce many parameters of inflammation and also to produce analgesia. The hypothesis will be tested that synthetic cannabinoids that activate the CB2 receptor can enhance the analgesic efficacy of opioids in the presence of inflammation by decreasing chemokines, immune mediators of inflammation.

Aim 2 will use a mouse model to determine whether exposure to either of the commonly used substances, nicotine and Δ^9-tetrahydrocannabinol (Δ^9-THC; the major psychoactive ingredient in

marijuana), alters responses to opioids. The hypothesis to be tested is that exposure to nicotine and Δ^9-THC during adolescence will produce heightened anxiety- and depression-like behaviors, reduce learning and memory, and increase opioid seeking. Further studies will test the hypothesis that the deleterious effects of Δ^9-THC are mediated by CB1, but not CB2, receptors. In both Aims, the systems will be dissected using agonist and antagonist cannabinoids that are selective for CB1 and CB2, and using mice with deletions of the CB2 receptor gene.

Principal Investigator

Toby K. Eisenstein, PhD
Professor and
Co-director, Center for Substance Abuse Research Center for Substance Abuse Research
Temple University School of Medicine
3500 N. Broad St.
Philadelphia, PA 19041

Other Participating Researchers

Martin W. Adler, PhD; Alan Cowan, PhD; Thomas J. Gould, PhD; Scott Rawls, PhD; Ronald Tallarida, PhD; Ellen M.Unterwald, PhD – employed by Temple University

Expected Research Outcomes and Benefits

This project will provide new and important information on the interactions of three major classes of addictive drugs, with the overall goal of improving treatment of substance abuse and pain. Overall, these studies will provide new and valuable information on drug interactions, including adverse drug interactions, as well as the possibility that some drug combinations could provide therapeutic advantages. By elucidating at a mechanistic level the interactions between opioids and synthetic cannabinoid drugs that selectively activate the CB2 receptor, the results could open new therapeutic modalities for pain management, thereby decreasing the potential liability of prescription opioid use while avoiding many of the adverse and medically undesired central nervous system effects associated with cannabinoids. Adolescence is a critical period in the initiation of drug use and development of addiction. While reasons for this are not well understood, nicotine and marijuana use may act as a gateway to other drugs, including opioids. The results of this project can guide policy in terms of information provided by government agencies to the public on the effects of combinations of drugs on their health. It is anticipated that the research proposed in this project will enhance our understanding of the neuronal circuits that are hijacked by abused substances, how the circuits for different drugs interact with each other, and how the neuronal endpoints targeted by these drugs are altered by products of the immune system. The results could have a significant impact on treatment of substance abuse and on development of new therapeutics for pain.

Summary of Research Completed

We have completed the initial work of hiring personnel, overseeing training, obtaining IACUC

and other Temple University- required approvals, ordering animals and receiving scheduled drugs. For Aim 1, it took several months to complete the process to hire a staff scientist and to obtain the IACUC approval.

Aim 1: *To determine the interactions of cannabinoids and opioids in terms of analgesia in two different pain models in rodents in the presence of inflammatory molecules produced by the immune system, called chemokines.*

Initial studies were undertaken to establish base-line responses to single drugs with known analgesic potency, morphine and the cannabinoid. WIN55212-2 (WIN). Dose-response curves were carried out to determine the effect of morphine and WIN on formalin-induced inflammatory pain model in mice. Morphine (0.5, 1, 3, 5 or 10 mg/kg) or saline was subcutaneously (sc) injected. At the same time, each mouse was injected sc into the dorsal surface of the left hind paw with 20 µl of a 5% formalin solution. Licking time was recorded at 20-35 min after formalin injection (Fig. 1A). A similar experiment was carried using WIN (0.5, 1, 1.5, 2 or 5 mg/kg) or saline (Fig. 1B). The data show that, as expected, morphine and WIN significantly decreased licking time ($p<0.01$, ANOVA followed by Tukey's test), in a dose-related manner, compared to the saline group, indicating an antinociceptive effect of both the opioid and the cannabinoid.

One aspect of this project is to collect tissue to analyze for chemokine/cytokine levels to correlate pain with inflammatory states and with the effect of the drugs on inflammation. Preliminary experiments were carried out to test procedures for measuring levels of chemokines in rodent tissue. Previous work in Dr. Eisenstein's laboratory had used blood or other fluids, not tissue, for measuring chemokines, and her standard assay technique only permitted determination of six analytes at a time. It was desired to use a multiplex technique that detected a larger number of analytes. Also, determining chemokine levels in tissues requires homogenizing and extracting the tissues in the presence of a protease inhibitor cocktail (Halt® Protease Inhibitor, Thermo Scientific). Banked, frozen samples of rodent tissue from historical experiments were used to test this extraction procedure. Samples were analyzed using the Proteome Profiler® Antibody Array (R&D Systems). This is a multiplex assay that detects 30 chemokines, cytokines and growth factors. Membranes supplied in the kit are blotted with the tissue extract and a cocktail of biotinylated detection antibodies. The array is developed with a streptavidin-horseradish peroxidase reagent followed by a Chemi Reagent Mix to produce chemiluminescence that can be quantitated using a Fuji Intelligent Dark Box II with Image Gauge® software (Fuji Film), This technique yielded visible, quantifiable spots on the membranes that correlated properly with treatment versus control, showing that it is a viable approach for screening for multiple chemokines/cytokines in tissues of treated animals. In addition, Dr. Eisenstein's laboratory has obtained access to, and learned the use of, a Luminex instrument for multiplex analysis of chemokines.

Aim 2: *To identify the long-term effects of nicotine and cannabinoid (Δ^9-THC) exposure during adolescence as compared with adulthood, on cognition, anxiety, depression and sensitivity to the effects of opioids using a pre-clinical mouse model.*

There are two sub-aims to this project. Both aims are designed to compare behavioral outcomes

when adolescent mice are exposed to nicotine as compared to adult mice, to assess the risk engendered by early exposure to this substance. In both sub-aims nicotine is given chronically to the mice and then administration is ceased (withdrawal). The effect of this prior exposure nicotine is being compared in adolescent versus adult mice, in sub-aim 2.1, for the effect on hippocampal-dependent and independent learning, using a fear-conditioning model. In sub-aim 2.2, the effect of prior nicotine exposure in adolescent mice is being examined in terms of a) depression-like behaviors using the forced swim test and b) on cocaine reward using the conditioned place preference procedure.

Methods: In both sub-aims, male C57BL/6J mice were obtained from Jackson Laboratory (Bar Harbor, ME). Nicotine administration began at 32 (periadolescent) or 54 (adult) days of age. Nicotine or saline vehicle was delivered by mini-osmotic pumps implanted subcutaneously at a dose of 12.6 mg/kg/day of nicotine for 12 days. After 12 days, the pumps were removed. In sub-aim 2.1, for fear conditioning, animals were trained and tested 30 days after nicotine withdrawal. Briefly, on the first day (day 30 post-withdrawal) animals were trained with a conditioned stimulus (85dB white noise) and an unconditioned stimulus (0.57 mA shock) for 2 CS-US pairings. Twenty-four hours after training animals were placed back into the fear conditioning chambers and freezing behaviors were assessed every ten seconds by an experimenter blinded to the treatment conditions. Approximately one hour later animals were assessed for their cued conditioning recall in an altered context and presented with the white noise for three minutes, while freezing behaviors were scored. For sub-aim 2.2, mice were tested after 24 hours or 30 days post-withdrawal. The forced swim test was used as a measure of depression-like behaviors. Briefly, mice were placed into clear cylinders containing 25°C water at a depth of 15 cm for 6 minutes, during which time behavior was video recorded. The amount of time the mouse spent immobile in the water (without active swimming or climbing) and the time for the mouse to first become immobile was measured. Rewarding effects of cocaine were measured in separate groups of mice after 24 hours and 30 days of nicotine withdrawal. During conditioning, mice received cocaine, 10 mg/kg, and were confined to the drug-paired chamber for 30 minutes. Five hours later, mice were injected with saline and placed in the opposite chamber for 30 minutes. After four days of conditioning, place preference was measured.

Results sub-aim 2.1. When adult mice were tested for altered hippocampal function after chronic adolescent administration of nicotine, they had lower freezing scores when tested in the context previously associated with a shock, compared to age-matched saline controls, $t(28) = 5.20$, $p < .001$. (Fig. 2) On the other hand, nicotine- and saline-treated animals did not differ on freezing behaviors when presented with the cue previously associated with a shock, $t(28) = 1.19$, $p = .25$. Taken together these results indicate that adolescent nicotine treatment creates long-term deficits in hippocampal-dependent learning while not altering hippocampus-independent learning.

Results sub-aim 2.2. In the first series of experiments, adolescent and adult mice given chronic nicotine were tested for depression-like behaviors 24 hours after cessation of nicotine administration. Results demonstrate that mice going through acute nicotine withdrawal exhibited increased depression-like behaviors as shown by higher immobility scores (Fig. 3A) and shorter latencies to immobility (Fig. 3B) compared to saline controls. Two-way ANOVA of immobility scores (1A) revealed a significant effect of nicotine treatment ($F(1,28)=30.57$, $p=0.001$) but no significant effect of age ($F(1,28)=0.91$, $p=0.54$). Posthoc analysis showed that nicotine exposure

resulted in significantly higher immobility time for the adolescent mice ($p<0.05$). Two-way ANOVA of latency to become immobile showed a significant effect of nicotine treatment ($F(1,28)=24.19$, $p=0.005$) and no significant effect of age ($F(1,28)=2.82$, $p=0.30$).

Nicotine administration during adolescence had long-lasting effects on depression scores. As shown in Fig. 4, mice that were exposed to nicotine as adolescents continued to show heightened depression-like behavior 30 days after cessation of nicotine administration (time immobile $p=0.0001$; latency to immobility $p=0.007$).

Mice were tested for the conditioned rewarding effects of cocaine after short-term and long-term withdrawal from nicotine administration. To test the effects of acute nicotine withdrawal, conditioning with cocaine began 24 hours after cessation of nicotine administration. Similar levels of cocaine place conditioning were found in mice exposed to nicotine as the saline control mice, as shown in Fig. 5. All mice developed a significant preference to the cocaine-paired environment, demonstrating cocaine reward. Place preference scores were not significantly different between treatment groups or ages. Similar results were found after long-term withdrawal from nicotine administration. Shown in Fig. 6 are the preference scores for mice that were exposed to nicotine as adolescents or adults followed by a 30-day withdrawal period. No significant effects of treatment or age of exposure were found.

These results demonstrate that nicotine withdrawal increases depression-like behaviors in mice as measured by immobility in the forced swim test. This phenotype persists into adulthood for mice exposed to nicotine in the adolescent period. Studies are underway to determine if similar effects are found when mice are exposed to nicotine as adults. The hypothesis is that heightened depression behaviors will persist after adolescent nicotine exposure but not adult nicotine exposure. Data from the place conditioning experiments show that nicotine exposure does not alter the rewarding effects of cocaine at a dose of 10 mg/kg in either age group. Studies have begun to test the rewarding effects of morphine using similar methods, as well as to test other doses of cocaine.

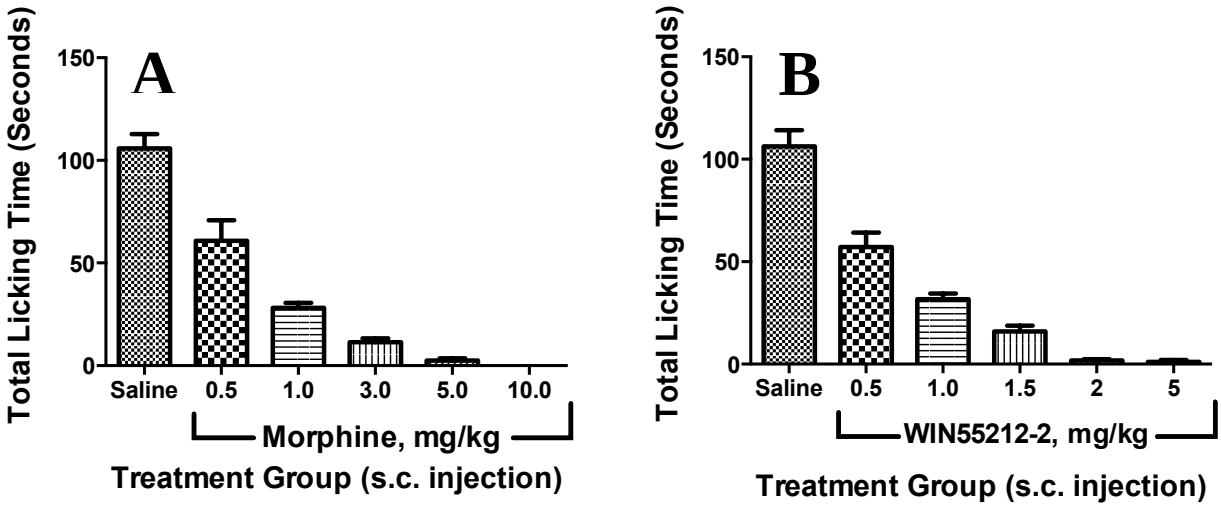

Figure 1. Dose-response curves for morphine (panel A) and WIN 55,212-2 (panel B) on formalin-induced nociception in mice. N=7-8 per group. Total licking time measured 20-35 min post-injection. Each point represents the mean ± SEM.

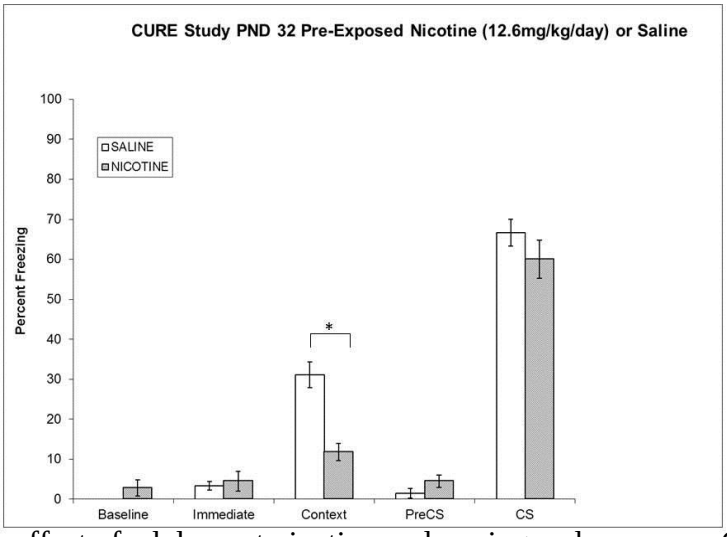

Figure 2: The effect of adolescent nicotine on learning and memory. Compared to saline controls, animals receiving adolescent nicotine showed lower percent freezing in contextual fear conditioning (*p < .001) but similar freezing scores in cued conditioning. Data shown are mean +/- SEM, n = 15/group.

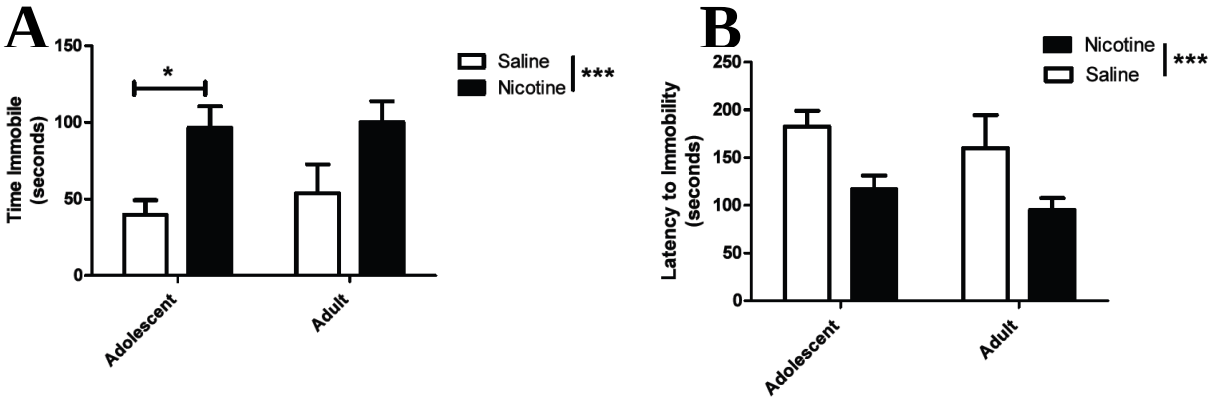

Figure 3 A. Time spent immobile. Nicotine administration significantly increased immobility times across age groups (two-way ANOVA) when tested after 24 hours of withdrawal (***p=0.001). Adolescent mice exposed for nicotine for 12 days spent more time immobile in the forced swim test than saline controls (*p<0.05). Data are shown as means + SEM, N=8/group. B. Latency to Immobility. Nicotine administration significantly shortened the latency to immobility across age groups (two-way ANOVA) when tested after 24 hours of withdrawal (*p=0.005). Data are shown as means + SEM, N=8/group.

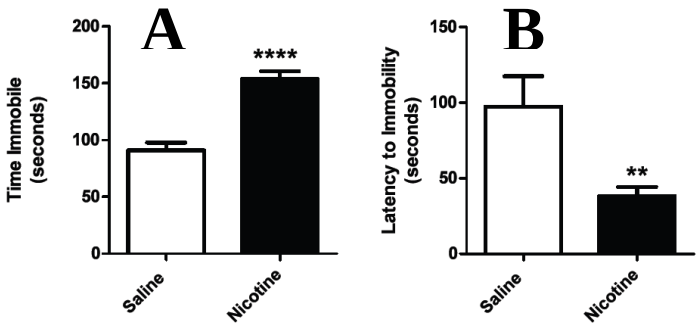

Figure 4. Immobility scores measured 30 days after withdrawal from chronic nicotine treatment during adolescence. Adolescent mice were exposed to nicotine for 12 days followed by 30 days of withdrawal. Time spent immobile (A) and latency to immobility (B) were significantly different in the nicotine treated mice (****$p<0.0001$; **$p<0.01$) indicating heightened depression-like behaviors after nicotine exposure. Data are expressed at mean + SEM, N=15-16/group.

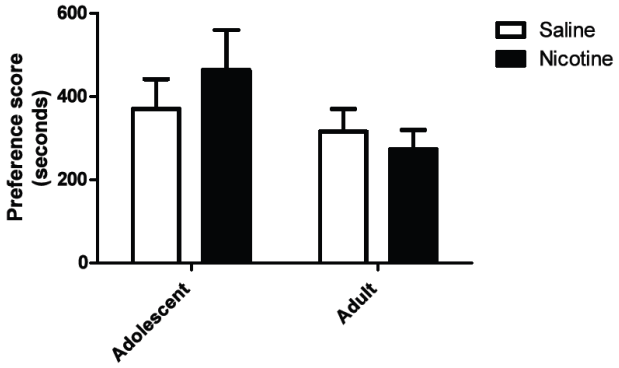

Figure 5. Cocaine conditioned place preference during short-term withdrawal from nicotine. Conditioning with 10 mg/kg cocaine resulted in a significant place preference for all groups of mice. There were no significant differences between ages or nicotine treatment. Data are shown as means + SEM, N=7-8/group.

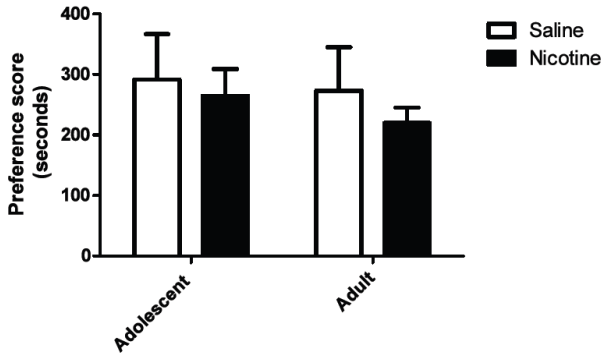

Figure 6. Cocaine conditioned place preference 30 days after withdrawal from nicotine. Conditioning with 10 mg/kg cocaine resulted in a significant place preference for all groups of mice. There were no significant differences between ages or nicotine treatment. Data are shown as means + SEM, N=7-8/group.